Environmental Research 220 (2023) 115093

Contents lists available at ScienceDirect

Environmental Research

journal homepage: www.elsevier.com/locate/envres

# Synergy of surface adsorption and intracellular accumulation for removal of uranium with *Stenotrophomonas* sp: Performance and mechanisms

Zhongqiang Hu [a,b], Zhongkui Zhou [a,b,**], Yaoyu Zhou [a,b,c,*], Lili Zheng [d], Jianping Guo [a,b], Yong Liu [a,b], Zhanxue Sun [a,b], Zhihui Yang [e], Xiaoxia Yu [a,b]

[a] State Key Laboratory of Nuclear Resources and Environment, East China University of Technology, Nanchang 330013, Jiangxi, China
[b] School of Water Resources and Environmental Engineering, East China University of Technology, Nanchang 330013, Jiangxi, China
[c] College of Resources and Environment, Hunan Agricultural University, Changsha 410128, China
[d] School of Energy and Environmental Engineering, University of Science and Technology Beijing, Beijing, 100083, China
[e] School of Metallurgy and Environment, Central South University, Changsha 410083, Hunan, China

ARTICLE INFO

*Keywords:*
Uranium
Wastewater
*Stenotrophomonas* sp. CICC 23833
Biosorption
Mechanism

ABSTRACT

Uranium is well-known to have serious adverse effects on the ecological environment and human health. Bioremediation stands out among many remediation methods owing to its being economically feasible and environmentally friendly. This study reported a great promising strategy for eliminating uranium by *Stenotrophomonas* sp. CICC 23833 in the aquatic environment. The bacterium demonstrated excellent uranium adsorption capacity ($q_{max}$ = 392.9 mg/g) because of the synergistic effect of surface adsorption and intracellular accumulation. Further analysis revealed that hydroxyl, carboxyl, phosphate groups and proteins of microorganisms were essential in uranium adsorption. Intracellular accumulation was closely related to cellular activity, and the efficiency of uranium processing by the permeabilized bacterial cells was significantly improved. In response to uranium stress, the bacterium was found to release multiple ions in conjunction with uranium adsorption, which facilitates the maintenance of bacterial life activities and the conversion of uranyl to precipitates. These above results indicated that *Stenotrophomonas* sp. Had great potential application value for the remediation of uranium.

## 1. Introduction

The huge energy demand of the world promotes the development of the nuclear industry, which inevitably leads to the massive exploitation of uranium (Bjorklund et al., 2017; Li and Zhang, 2012). At present, more than 40 billion tons of uranium ore have been produced worldwide, along with as many as 20 billion tons of tailings (Nair et al., 2010; Kamunda et al., 2016). Exposed waste rock and tailings are continuously leached by rain and weathering, causing the release of uranium compounds into nearby soil and groundwater and subsequent uranium entry into the ecological food chain (Saueia and Mazzilli, 2006; Ashrap et al., 2020). When the accumulated radionuclides in the body exceed a certain limit, they may cause leukemia, cancer, and heavy metal ion poisoning (Ashrap et al., 2020; Milacic et al., 2004; Wagner et al., 2010). Therefore, the prevention and control of uranium pollution have become an urgent problem.

At present, the main treatment methods for uranium-containing wastewater include physicochemical remediation and bioremediation. Uranium-containing wastewater has extensive research in physicochemical remediation. For example, Wang et al., (2022) found that uranium's removal rate and adsorption capacity by acidified sodium feldspar was 84.9% and 0.52 mg/g at pH = 6. Waqas Ahmed et al., (2021) used the hydroxyapatite biochar nanocomposite and could reach a maximum adsorption capacity of 423.04 mg/g for uranium within 30 min. The physicochemical methods were shown to be effective in the treatment of uranium-containing wastewater, but there are still problems such as high material and site costs and serious secondary pollution (Zhang et al., 2014; Ishag et al., 2020). Thus, bio-derived adsorbents have received increasing attention for wastewater treatment (Banala and Subba Rao Toleti, 2021).

Compared with traditional physicochemical methods, microbiological methods are deemed environmentally friendly, highly efficient, and

* Corresponding author. College of Resources and Environment, Hunan Agricultural University, Changsha, 410128, China.
** Corresponding author. School of Water Resources and Environment Engineering, East China University of Technology, 330105, China.
*E-mail addresses:* zhkzhou80@163.com (Z. Zhou), zhouyy@hunau.edu.cn (Y. Zhou).

https://doi.org/10.1016/j.envres.2022.115093
Received 14 November 2022; Received in revised form 10 December 2022; Accepted 15 December 2022
Available online 24 December 2022

cost-effective (Sharma et al., 2016; Wang, 2002). Previous studies of microbiological methods' removal effects and performance confirm its promising potential for uranium removal (Liu et al., 2021; Sivaperumal et al., 2022). The microbiological immobilization of uranium primarily consists of four mechanisms: biosorption, biomineralization, bioreduction, and bioaccumulation (Manobala et al., 2019). Among them, biosorption has attracted wide attention because of its excellent economic feasibility and high treatment efficiency. The abundance of organic groups on bacterial cell surfaces (such as amino, carboxyl, phosphate, and hydroxyl groups) were significant components for microbe-uranium interactions (Lutke et al., 2012; Zou et al., 2014).

As for specific bacteria, Barnali Sarma et al. (Sharma et al., 2016) found that pseudomonas fluorescent could remove up to 94% of the uranium in an environment with a uranium concentration of 100 μM. Suzuki et al. (Suzuki and Banfield, 2004) treated uranium-containing solutions with bacillus subtilis and adsorbed up to 160 mg/g in 1 h. However, most analyses and studies of bacterial adsorption processes are limited and mainly focus on the extracellular adsorption and extracellular precipitation of microorganisms. There are still few reports exploring the intrinsic relationship between uranium adsorption and ion release from the bacterium, and there is also a gap in the field of improving the ability of bacterial intracellular accumulation. *Stenotrophomonas* sp. CICC 23833 has the advantage of excellent effectiveness and short consumption time in the treatment of uranium-containing wastewater, which involves both extracellular adsorption and intracellular accumulation, as well as a certain mechanism of uranium detoxification.

Herein, this study aimed to investigate the uranium adsorption by *Stenotrophomonas* sp. In water and explored the possible adsorption mechanisms. We have examined the uranium adsorption capacity of the bacterium under different adsorption conditions; analyzed the link between uranium adsorption behaviour and the ion release behaviour of the bacterium; identified the functional groups of bacteria that involving in adsorption; tested the uranium handling capacity of bacterial permeabilized cells and located of uranium after its accumulation by bacterial cells. This study provides a theoretical basis and technical support for the treatment of uranium-contaminated wastewater.

## 2. Materials and methods

### 2.1. Reagents

The reagents used in the experiments were of analytical grade. Triton-100 and Tween 80 were purchased from Jinclon Biotechnology Co., Ltd. Pentanediol was purchased from Maclean's. $U_3O_8$ was purchased from the Beijing Institute of Metallurgy, Nuclear Industry.

### 2.2. Bacteria and bacterial culture

The strain used in this experiment was *Stenotrophomonas* sp. CICC 23833 was purchased from the China Industrial Microbial Strain Conservation Center (CICC), and the storage method was refrigerator freezing at −80 °C.

The bacteria were incubated in Luria Broth (LB) medium at 30 °C and shaken at 120 rpm (Desai et al., 2008). After 36 h of incubation, the bacteria were collected by centrifugation at 4 °C for 5 min at 6000 rpm and then washed three times with sterile deionized water to obtain the bacterial cells. The obtained bacterial cells will be used in the following experiments. (1) The bacterial cells were freeze-dried and the dry weight of the bacteria was calculated. (2) The washed bacterial cells were dissolved in sterile water to prepare a concentration of cell suspension for subsequent adsorption, inactivation, permeation, and uranium stress response experiments (Ge et al., 2015; Yu et al., 2022).

### 2.3. Characterization of bacteria

Bacterial adsorption experiments were performed at, cell concentration of 0.2 g/L, initial uranium concentration of 50 mg/L, 30 °C, pH = 6, and 120 r/min. After adsorption, the bacterial precipitate was obtained by centrifugation at 6000 rpm for 10 min. The bacterial precipitates obtained were used for the following analyses. (1) Analysis of surface morphology and chemical element composition of bacteria from before and after adsorption. (2) Analysis of the internal ultrastructure and chemical elemental composition of bacteria from before and after adsorption. (3) Analysis of functional groups of bacteria from before and after adsorption.

### 2.4. Uranium adsorption experiments

Uranium adsorption experiments on bacteria were carried out at a cell concentration of 0.2 g/L, initial uranium concentration of 50 mg/L, 30 °C, pH = 6, and 120 r/min. Sampling was carried out at different times (0–8 h) to determine the effect of adsorption time on the effectiveness of bacterial uranium treatment. The system was adjusted to different pH values (3–8) to determine the optimum pH for bacterial uranium adsorption. Different initial uranium concentrations (10–150 mg/L) were adjusted to investigate the effect of different initial uranium concentrations on uranium adsorption by the bacteria. The effect of temperature on uranium adsorption by the bacterium was examined by adjusting the incubation temperature (20–40 °C).

### 2.5. Analysis of uranium removal capacity of inactivated and permeable bacteria

They were prepared as follows: (1) The cell suspensions were fixed with 2.5% glutaraldehyde for 24 h to obtain glutaraldehyde-treated bacteria (Huang-LeeLlh and Nimni, 2010; Ramrakhiani et al., 2016; Deng and Ting, 2005). (2) The prepared bacterial suspension was inactivated at 121 °C for 20 min in an autoclave to obtain high-temperature-inactivated organisms (Wang et al., 2017). (3) The permeabilized bacteria were obtained by adding 0.2% (v/v) Triton X-100 and 0.2% (v/v) Tween 80 to the cell suspension and vortexing for 20 min (Desai et al., 2008; Soni et al., 2013).

Take appropriate amounts of the bacteria treated by the above process and add them to 50 mg/L uranium solution to make the cell concentration 0.2 g/L. Adsorption was carried out at 30 °C, 120 r/min, and sampled at different times (0–8 h).

### 2.6. Analysis of bacterial response mechanism to uranium stress

An appropriate amount of the cell suspension prepared by the method of 2.2 was added to 50 mg/L of uranium solution to achieve final concentrations of 0, 0.01, 0.02, 0.04, 0.1, 0.2, and 0.4 g/L respectively. Adsorption at 30 °C and 120 r/min for 4 h. The solution was centrifuged at 6000 r/min for 10 min and filtered through a 0.22 μm membrane to obtain a supernatant sample.

### 2.7. Characterization analysis

$K^+$, $Ca^+$, $Na^+$, $NH_4^+$, $Mg^{2+}$, and $U^{6+}$ were determined by an inductively coupled plasma emission spectrometer (Agilent 5100 ICP–OES). $NO_3^-$, $Cl^-$, $NO_2^-$, $SO_4^{2-}$, and inorganic phosphate were determined by ion chromatography (ISP-1100). The bacterial surface morphologies of the samples were observed by scanning electron microscopy (SEM, Nova Nano SEM 450) combined with Energy dispersive spectroscopy (EDS) to analyze their chemical elemental compositions. Transmission electron microscopy (TEM, FEI Tecnai Spirit) was used to obtain the bacterial cells' overall morphology and internal ultrastructure. Fourier infrared spectroscopy (FTIR) patterns were determined by the Thermo Nicolet 6700 instrument.

## 3. Results and discussion

### 3.1. Characterization of Stenotrophomonas sp.

#### 3.1.1. SEM-EDS and TEM analysis of Stenotrophomonas sp.

SEM-EDS and TEM analyses were used to determine the cellular location of uranium after adsorption. The morphology of the cells did not change significantly compared to the bacterial cells treated before adsorption (Fig. 1a and b), but the bacteria treated with uranium solution showed distinct uranium characteristic peaks. Some research has explained this phenomenon as some organic material secreted by extracellular bacteria, which forms a precipitate with uranium on the cell surface (Morel et al., 2009; Pinel-Cabello et al., 2021).

Transmission electron microscopic analysis indicated that no unidentified material was seen in the cells before uranium adsorption (Fig. 2a and b). The appearance of long black opaque stripes inside the cells exposed to uranium solution, combined with the results of intracellular EDS dot analysis (Fig. 2c and d), indicated the presence of uranium inside the cells and coincided with the distribution of P, S elements inside the cells (Fig. 2e–i). Thus, the adsorption of uranium by *Stenotrophomonas* sp. Was a combination of extracellular adsorption and intracellular accumulation. Similar results were observed by Iv'an S'anchez-Castro and Pinel-Cabello et al. (Sanchez-Castro et al., 2021; Pinel-Cabello et al., 2021).

#### 3.1.2. FTIR spectra of Stenotrophomonas sp.

Microbial adsorption includes various processes, such as extracellular adsorption and intracellular adsorption, and the effect of extracellular adsorption is closely related to the functional groups on the surfaces of the microbes. Therefore, the identification of the functional groups involved in the extracellular adsorption of uranium was necessary. As shown in Fig. 3, the bands at 3428.5 and 2962.6 $cm^{-1}$ correspond to the O–H and N–H stretching vibrations (Yi et al., 2017) and the antisymmetric stretching vibration of alkane C–H, respectively (Ye et al., 2013). The peak near 1402.3 $cm^{-1}$ can be attributed to the amino acid C–N or terminal carboxyl vibration (Jain et al., 2009; Han et al., 2007), while the peaks near 1243.3 and 1077.5 $cm^{-1}$ indicated the presence of phosphate groups (Yu et al., 2022). The peaks of 3425.1 and 2960.6 $cm^{-1}$ after the adsorption of uranium compared to before adsorption indicate the involvement of –OH and $–NH_2$ groups in the adsorption of uranium (Yi et al., 2017). The peak at 1394.7 $cm^{-1}$ is associated with the $–NH_2$ and –COOH stretching vibrations (Cheng et al., 2021), which combined with the release of $NH^{4+}$ during the adsorption of uranium, indicated the involvement of macromolecules such as proteins in the adsorption process. The peak variations of 1242.6 and 1077.5 $cm^{-1}$ were attributed to the weakening of the vibrations of the phosphate groups P═O and P–O after uranium loading (Yu et al., 2022). Furthermore, the presence of an inorganic phosphate group released during uranium adsorption by the bacterium indicates that lipids are also involved in the uranium adsorption process (Gerber et al., 2018) (see Fig. 4).

### 3.2. Uranium adsorption performance

#### 3.2.1. Effect of contact time

Studies have reported that to resist the chemical toxicity of uranium, microorganisms will produce various substances, such as polyphosphates, under uranium stress (Achbergerová and Nahálka, 2011). Therefore, the adsorption time of the bacteria also has a significant impact on the treatment effect, which is related to not only the contact time between the functional groups and uranyl ions but also the state of the bacteria under uranium stress (Bondici et al., 2015). It can be seen from Fig. S1 that the adsorption of uranium by bacteria occurs mainly in the first 0.5 h, which is similar to the reported behaviour of uranium adsorption by other microorganisms (Jing et al., 2011), and the bacteria will reach adsorption equilibrium within 4 h, and the biosorption capacity is 174.32 mg/g. Compared to the treatment time of Iván Sánchez-Castro et al. (Sanchez-Castro et al., 2021) using *Stenotrophomonas strain Br8*, this bacterium has a faster treatment rate, which means it has a shorter hydraulic residence time. No significant desorption occurred within 24 h. Therefore, *Stenotrophomonas* sp. Has a more stable treatment effect on uranium in water bodies.

#### 3.2.2. Effect of pH

The pH could significantly influence the ionization states of functional groups on the biomass surface and the solubility of metal ions, thereby exerting some effects on the adsorption process (Sharma et al., 2016). It can be seen from Fig. 5a that the optimum adsorption pH of this bacterium was 6, and the biosorption capacity reached 174.32 mg/g at 3 h. Fig. 5b showed that the environmental pH tends to change to neutral

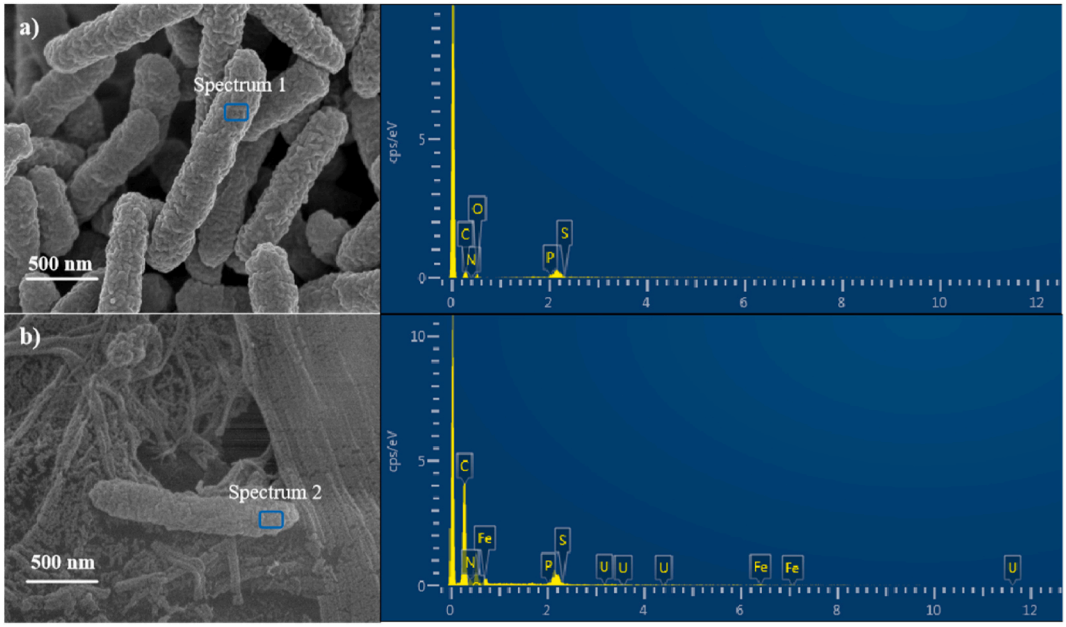


**Fig. 1.** SEM-EDS of *Stenotrophomonas* sp. Before (a) and after (b) uranium biosorption.

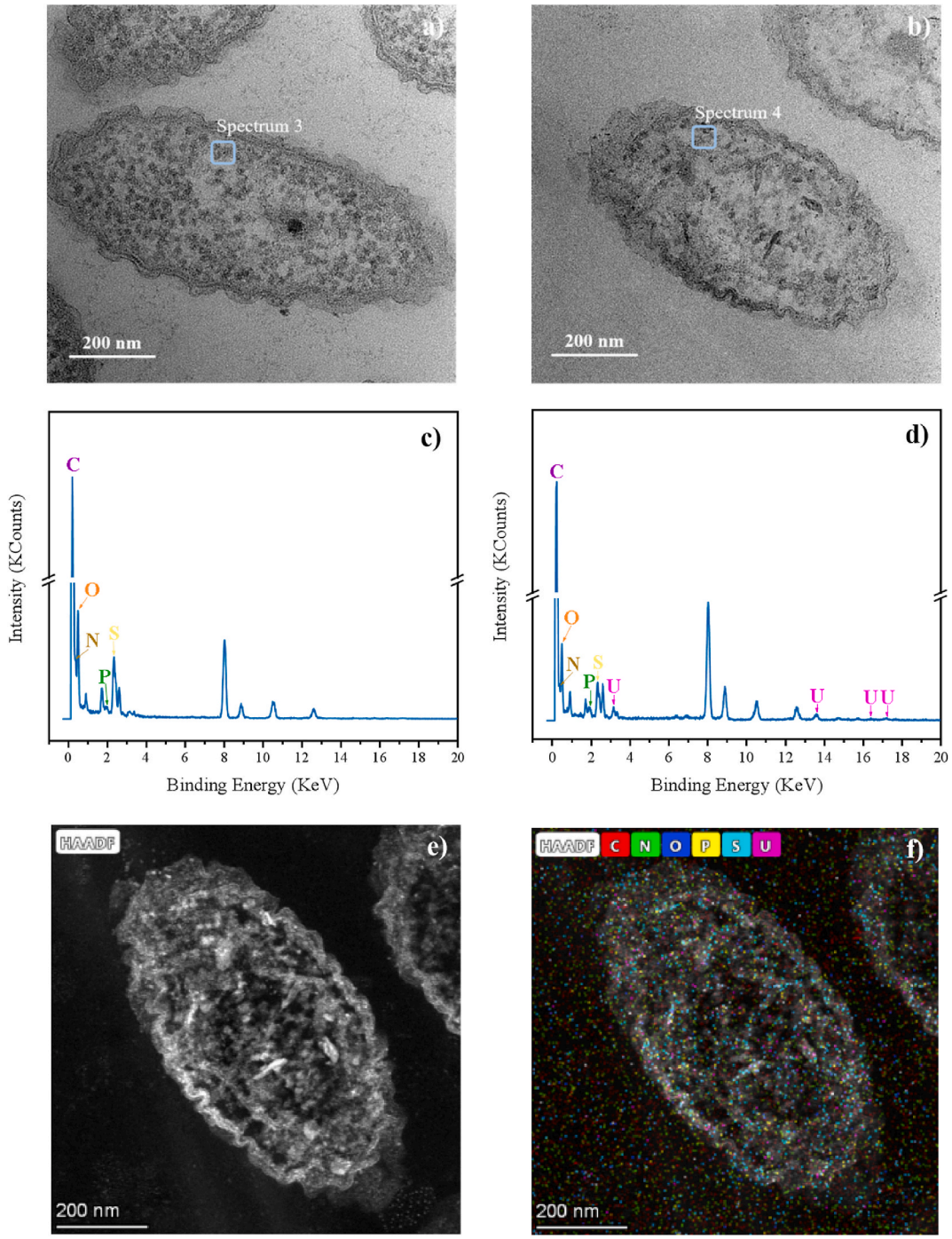


**Fig. 2.** TEM images of *Stenotrophomonas* sp. (a) and (b) SEM of *Stenotrophomonas* sp. Before and after exposure to uranium. (c) and (d) Scanning EDS spectra of points 3 and 4 in TEM image (a) and (b). (e) To (i) Corresponding EDS mapping images of *Stenotrophomonas* sp. Exposure to uranium.

after adsorption for different initial pH conditions. Uranium adsorption was highest at pH 6 and the pH increase was larger. This is due to the different cell viability under different pH conditions. Therefore, it can be speculated that bacteria have some ability to regulate the pH of the external environment, Marqués and Ednei Coelho's came to a similar conclusion (Marqués et al., 1991; Coelho et al., 2020). This process is associated with the emission of phosphate, which helps bacteria cope with the toxicity caused by uranyl ions (Pinel-Cabello et al., 2021). In addition to affecting microbial activity, pH can also influence the fugitive form of uranium. At low pH, $H^+$ competes with uranyl ions for binding sites on the bacterial surface (Yang and Volesky, 1999), and at pH = 7, uranium was mainly present as $(UO_2)_3(OH)^{5-}$ and $UO_2(OH)_2$ (aq), indicating that microorganisms have a good adsorption effect on uranium-containing compounds in this form (Zhang et al., 2018).

### 3.2.3. *Effect of initial uranium concentration*

The initial concentration of uranium was a significant factor affecting the biosorption capacity and efficiency of the bacterium. As shown in Fig. 6, the biosorption of uranium was proportional to the initial uranium concentration, while the adsorption efficiency exhibited an opposite trend. This was because the bacterium had a large number of binding sites and did not reach saturation, with increasing uranium

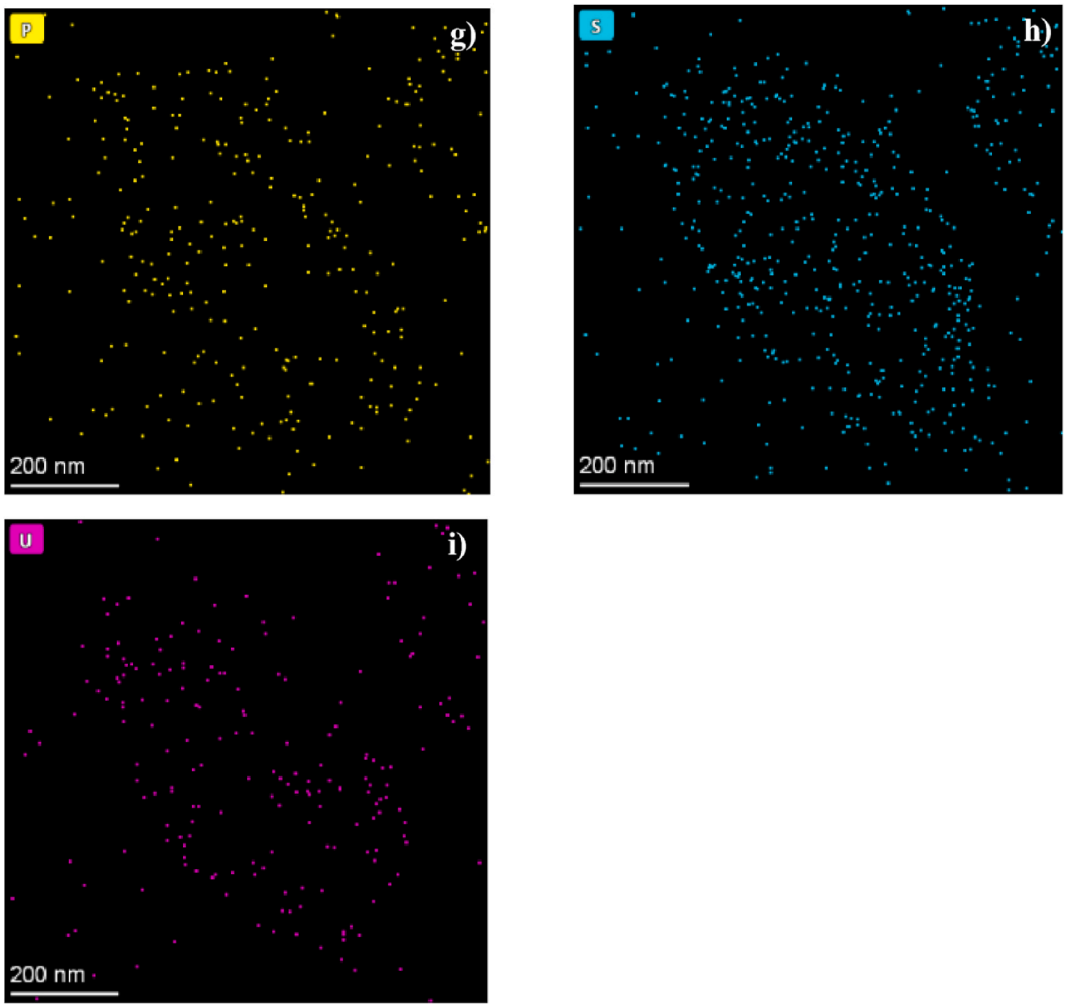


**Fig. 2.** (*continued*).

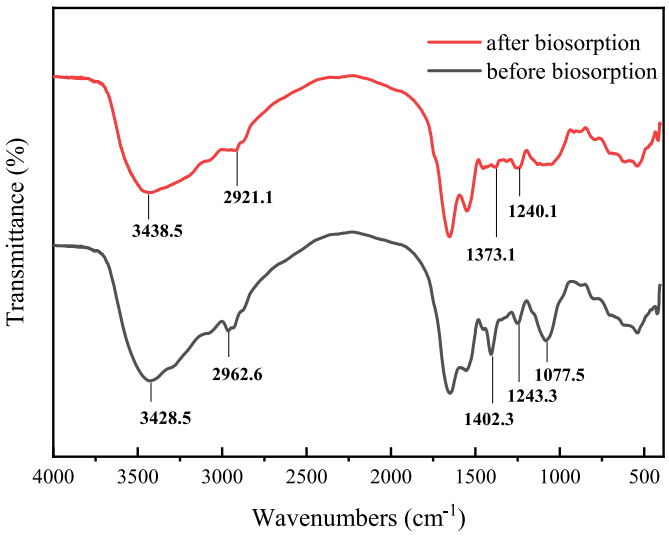


**Fig. 3.** FTIR images of *Stenotrophomonas* sp. Before and after biosorption.

concentration, a growing number of uranium ions in solution were bound by the binding sites of the bacterium, thus increasing the biosorption capacity. As the uranium concentration increased from 10 to 150 mg/L, the uranium adsorption capacity of the bacteria increased from 43.7 to 392.9 mg/g. However, as the concentration of uranium increases, the proportion of available binding sites in the bacterium becomes smaller, and more uranium ions are in a free, unbound state, leading to a decrease in the adsorption efficiency (Tunali et al., 2006).

### 3.2.4. Adsorption kinetic equation

Fig. 7 and Table S1 show that the fitting coefficient of quasi-second-order kinetics ($R^2 > 0.998$) was higher than that of quasi-first-order kinetics ($R^2 > 0.954$). Furthermore, the theoretical adsorption capacities (82.82–110.00 mg/g) of the quasi-first-order kinetic model differed significantly from the experimentally obtained adsorption capacities (206.5–217.1 mg/g). The theoretical adsorption capacities calculated by quasi-second-order kinetic equations (175.44–209.21 mg/g) were much closer. This indicated that the uranium adsorption process was more consistent with the quasi-second-order kinetic equation under different influencing factors, suggesting that the ability to adsorb uranium depends on the active site available to the bacterium and the concentration and nature of uranium in solution (Li et al., 2016).

### 3.2.5. Adsorption isotherm equation

The adsorption isotherm model fitting results are shown in Fig. S2 and Table S2. The correlation coefficient of the Freundlich model was 0.996, which was higher than that of the Langmuir model (0.966), indicating the uranium adsorption process by *Stenotrophomonas* sp. Was a heterogeneous surface adsorption process. Moreover, the adsorption of uranium by *Stenotrophomonas* sp. Is a heterogeneous surface adsorption process (Tunali et al., 2006). Its theoretical saturation biosorption

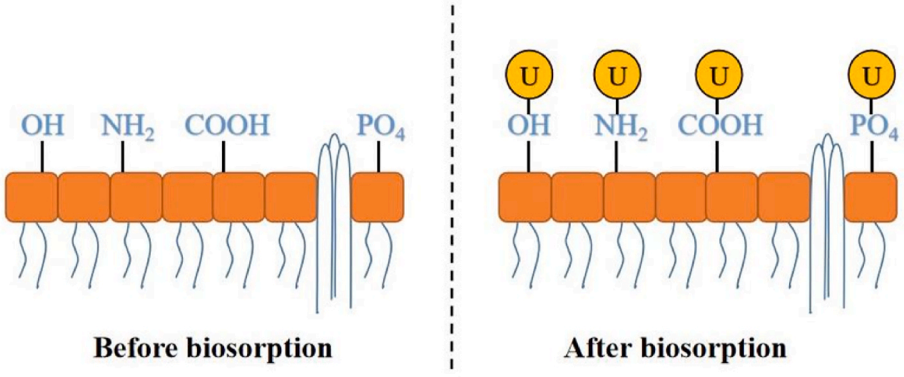


**Fig. 4.** Schematic diagram of uranium-adsorbing functional groups on the surface of bacteria.

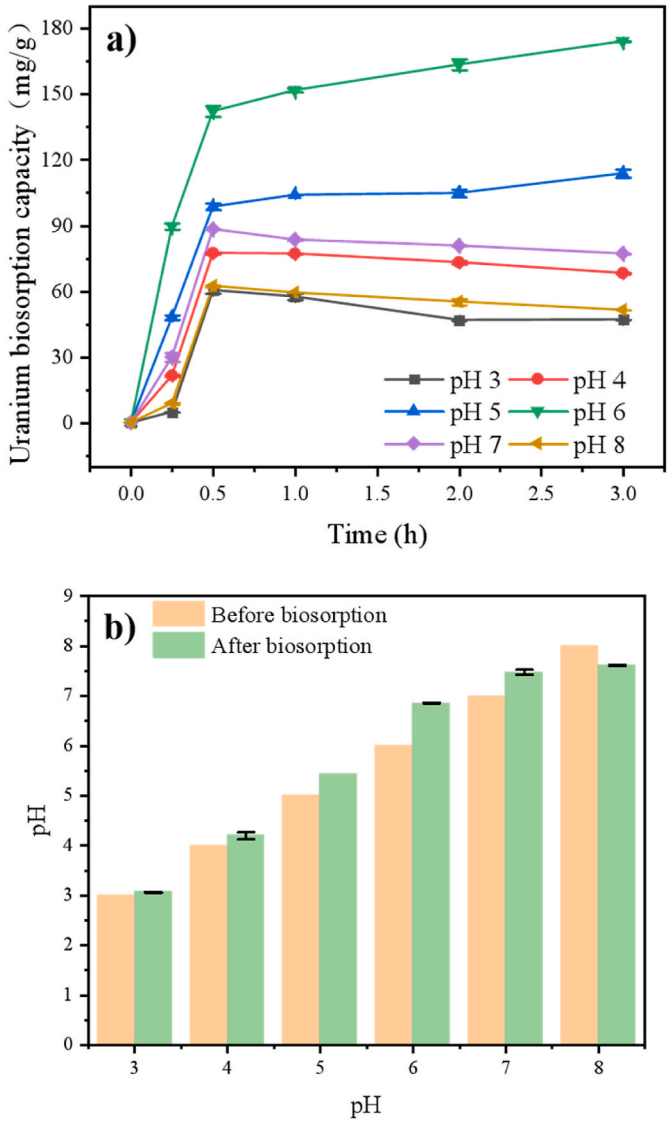


**Fig. 5.** Changes in biosorption capacity (a) and pH (b) with time under different pH conditions.

capacity for uranium was 301.20 mg/g. Compared with other microbial adsorption studies (Table S3), it shows great advantages (Coelho et al., 2020; Manobala et al., 2019; Wang et al., 2017).

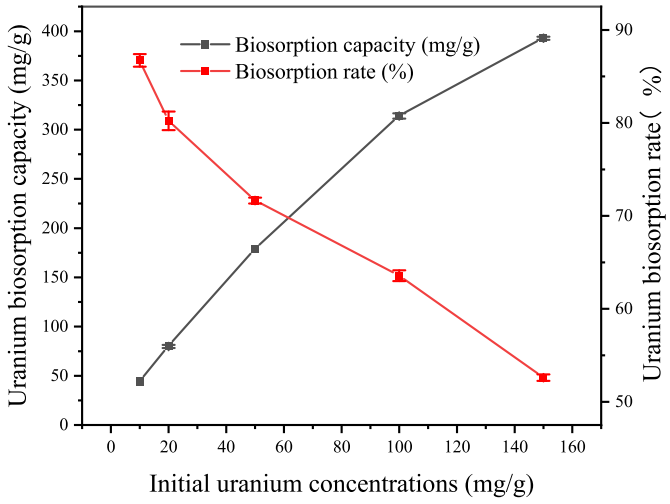


**Fig. 6.** Uranium biosorption capacity and rate exhibited by bacteria at different initial uranium concentrations.

### 3.3. *Uranium removal by inactivated and permeable bacteria*

#### 3.3.1. *Effect of inactivation treatment*

The intracellular accumulation of substances by bacteria is an energy-consuming process (Banala and Subba Rao Toleti, 2021). Therefore, to investigate the relationship between intracellular accumulation and bacterial activity, this experiment investigated the contribution of surface adsorption, intracellular accumulation, cellular activity, and cell structure to bacterial adsorption of uranium by two methods of inactivation, at 121 °C and glutaraldehyde. The adsorption of high-temperature-inactivated bacteria at 0–2 h was higher than that of other bacteria (Fig. 8), which was similar to the comparative results of the adsorption of metals by other microbial cells (Mohamed, 2001). After 4 h, the adsorption of the blank group was higher than that of the inactivated bacteria, while the adsorption of the glutaraldehyde-inactivated treated bacteria was always at a lower level. This was because the adsorption of uranium by bacteria relies on the second stage of intracellular accumulation behaviour in addition to the first stage of extracellular adsorption (Banala and Subba Rao Toleti, 2021; Deng and Ting, 2005). In contrast to heat inactivation, glutaraldehyde can be used for cell inactivation while preserving the cell structure and functional groups on the surface of the bacterium. However, the ability of inactivated organisms to process uranium was lower than that of normal organisms, regardless of whether they had an intact cellular structure, again demonstrating the contribution of intracellular accumulation to bacterial uranium processing and showing that intracellular transport is inextricably linked to cellular activity (Lee and Hur,

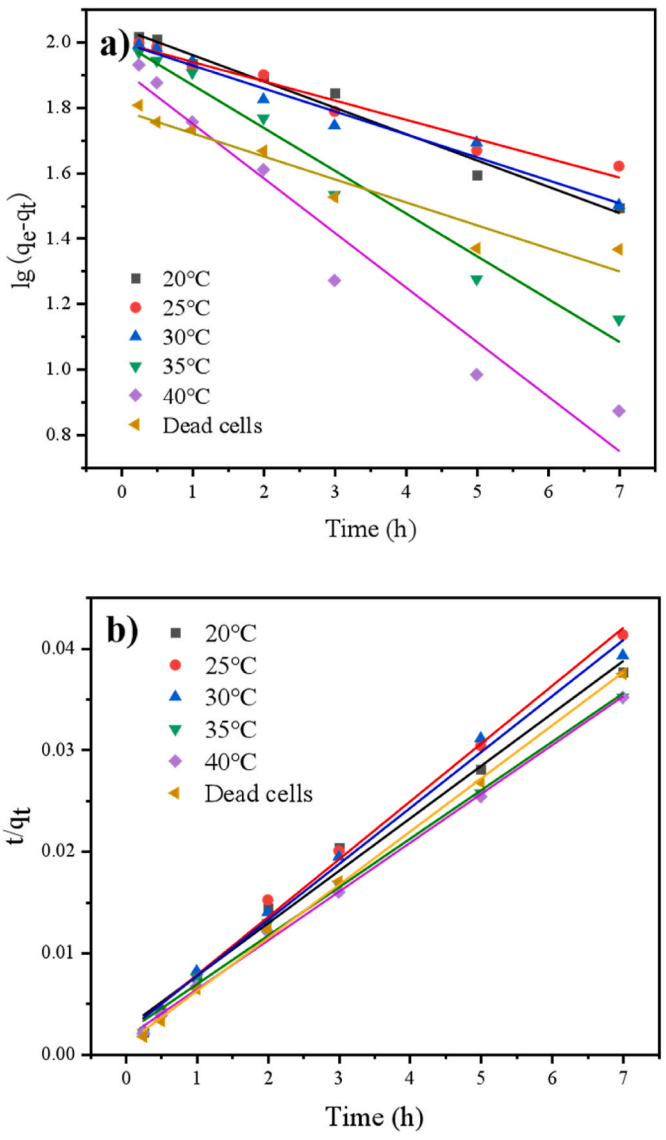


**Fig. 7.** Pseudo-first-order model and pseudo-second-order model for the adsorption of uranium by *Stenotrophomonas* sp.

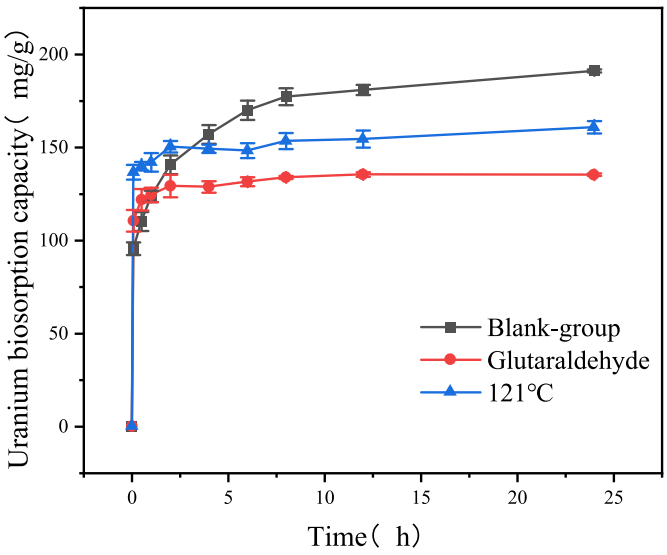


**Fig. 8.** Changes in biosorption capacity by live cells and dead cells over time.

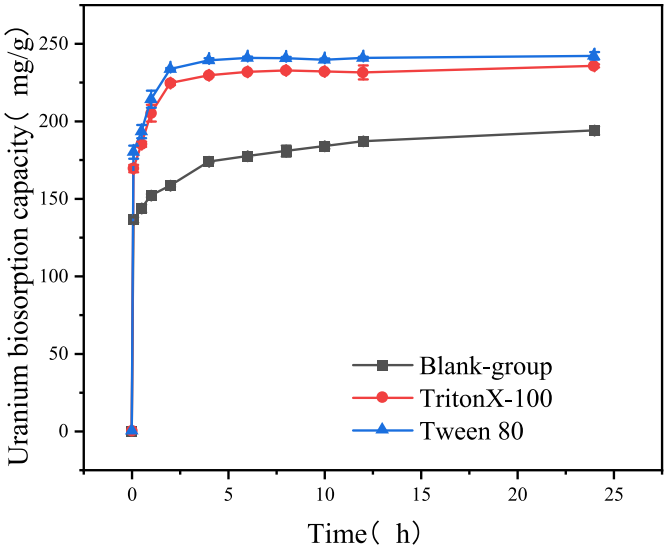


**Fig. 9.** Changes in the uranium biosorption capacities of permeabilized cells with time.

2014; Huang et al., 2020; Pan et al., 2015).

### 3.3.2. *Effect of permeabilization treatment*

With continuous research, it was found that by increasing the permeability of the cells, the adsorption effect was greatly improved (Ge et al., 2015). As shown in Fig. 9, the adsorption speed decreased after 0.5 h. Uranium ions gradually entered the cell interior through active transport, and the adsorption rate of the permeabilized bacteria was still significantly higher than that of the blank group. This was because permeabilizes increase the permeability of cells and help them release cytoplasmic soluble proteins to translocate uranium ions into the cells. The release of cytoplasmic soluble proteins increased the contact between uranium ions, which allowed permeabilized bacteria to reduce uranium ions more effectively (Sumit and Alok, 2013; Sultan and Hasnain, 2007). At 24 h, the adsorption capacities of the bacteria pre-treated with 0.2% (v/v) Triton X-100 and 0.2% (v/v) Tween 80 reached 235.7 mg/g and 242.2 mg/g for uranium, with adsorption rates of 94.28% and 96.88%, respectively, which were 21.5% and 24.9% higher than the adsorption capacity of the normal bacteria. Therefore, the permeabilized bacteria can treat uranium ions in wastewater more effectively than ordinary bacteria, and the intracellular adsorption of the bacteria has a greater potential to be enhanced, for which Tween 80 is the most effective permeabilizer (Desai et al., 2008).

### 3.4. *Mechanisms of bacterial response to uranium stress*

Bacteria respond to uranium stress by producing multiple changes (Achbergerová and Nahálka, 2011). To investigate the bacterial coping strategies in uranium-containing environments and the characteristic mechanisms of uranium adsorption, we examined the concentrations of various ions in solution and found that bacterial adsorption of uranium is accompanied by a series of ion-releasing behaviours (Fig. 10 and Fig. S3). The first was attributed to changes in the external environment, thus resulting in the release of ions from the bacterium into the solution to alleviate the difference in osmotic pressure inside and outside the cell. Second, during uranium biosorption, certain ions are exchanged (Yi et al., 2017). To understand the relationship between uranium adsorption and ion release, we performed a correlation analysis of uranium adsorption with the concentration of each ion in the solution. The results of the analysis showed (Table 1) that uranium adsorption was

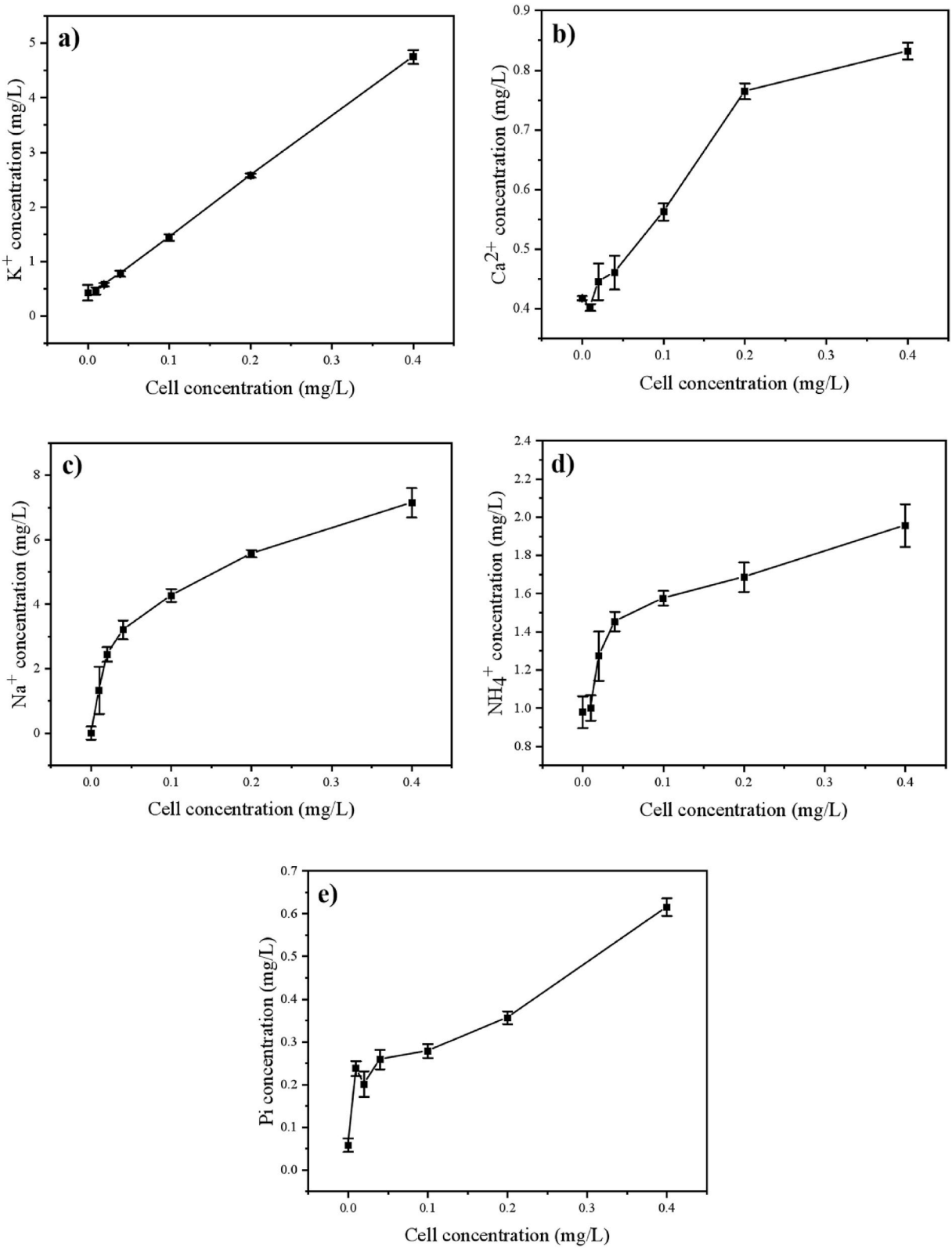


**Fig. 10.** Release of ions after uranium biosorption by *Stenotrophomonas* sp. (a) Potassium ion. (b) Calcium ion. (c) Sodium ion. (d) Ammonium ion. (e) Inorganic phosphate group (pi).

significantly and positively correlated with the release of $K^+$, $Ca^{2+}$, $Na^+$, $NH_4^+$, $NO_2^-$, $SO_4^{2-}$ and inorganic phosphate group (pi) and negatively correlated with the release of $Mg^{2+}$ and $NO_3^-$ (see Fig. 11).

Among them, the release of $Na^+$ and $K^+$ was related to the utilization of $Na^+$ and $K^+$-ATPase. Pribil et al. (Pibil et al., 1975) showed that the transmembrane transport of uranium requires the participation of ATP and that $K^+$ is an important enzymatic activator in ATP synthesis and respiration (Vieira et al., 2019). These results again suggested that $K^+$ release was associated with bacterial uranium adsorption, which was also observed for other microorganisms with heavy metal removal

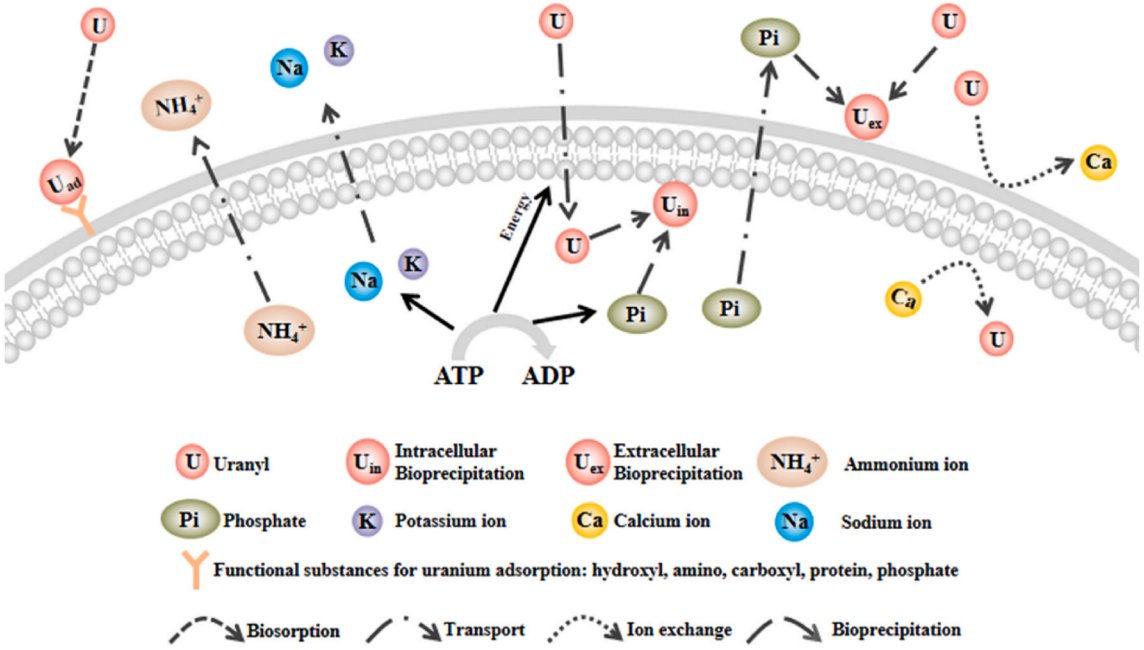


**Fig. 11.** The possible schematic diagram of uranium stress resistance mechanisms and uranium adsorption in *Stenotrophomonas* sp.

**Table 1**
Correlation between uranium adsorption and ion release by *Stenotrophomonas* sp.

| | P | | P |
|---|---|---|---|
| $K^+$ | 0.922** | $Cl^-$ | −0.260 |
| $Ca^{2+}$ | 0.932** | $NO_2^-$ | 0.969** |
| $Na^+$ | 0.992** | $SO_4^{2-}$ | 0.920** |
| $Mg^{2+}$ | −0.943** | $NO_3^-$ | −0.973** |
| $NH_4^+$ | 0.958** | $PO_4^{3-}$ | 0.973** |

1) * for P < 0.05 , ** for P < 0.01.

capacities (Ye et al., 2013). The conversion of ATP to ADP will cause the release of Pi, which is one of the reasons for bacterial alkaline production (Zheng et al., 2017). The SEM and FTIR results also indicated the greater contribution of phosphate groups in the surface adsorption of uranium (Sanchez-Castro et al., 2020), which promoted the chelation of uranium with phosphate groups and reduced the toxicity of uranium in solution (Shen et al., 2018). The TEM results also indicated that phosphate groups play a critical role in promoting the formation of intracellular uranium precipitates. This is a mechanism of bacterial resistance to uranium stress and a similar strategy was observed in *P. stutzeri* and algal cells (Yu et al., 2022; Choudhary and Sar, 2011). The release of $NH_4^+$ occurs because when bacteria are in an external nutrient-free environment, they break down intracellular organic matter for endogenous respiration to obtain energy to meet their energy requirements for survival, which leads to the release of $NH_4^+$ (Hao et al., 2009). $Ca^{2+}$ is released due to the ion exchange phenomenon between uranium and $Ca^{2+}$ (Yi et al., 2017). The release of ions is a manifestation of the bacteria's adaptation to the uranium-containing environment. The bacteria used in this study demonstrated high tolerance to the uranium environment, which supports the application of the strain in the remediation of uranium contamination.

## 4. Conclusions

This research investigated *Stenotrophomonas* sp. Processes for high-efficiency uranium adsorption. The adsorption capacity of the bacterium for uranium was achieved at 194 mg/g. Based on the results of SEM, TEM, adsorption isotherms, and kinetic fitting, we found that uranium was distributed on the surface and inside of the bacterial cells after adsorption, indicating the occurrence of active transport during uranium adsorption. The adsorption rate and adsorption capacity of the bacteria treated by permeabilization could reach 96.88% with 242.2 mg/g, which improved the adsorption efficiency by 24.9%. The opposite result was obtained with glutaraldehyde treatment, which again proved the intracellular accumulation of the bacterium and its high potential. The uranium adsorption behaviour of the bacteria was found to be associated with the release of $K^+$, $Ca^{2+}$, $Na^+$, $NH_4^+$, $NO_2^-$, $SO_4^{2-}$, and $PO_4^{3-}$. This demonstrates the involvement of $Na^+$, $K^+$-ATPase, the release of Pi, the endogenous respiration of bacteria, and the ion exchange behaviour of uranium and $Ca^{2+}$ during uranium adsorption. The results of this study indicated that *Stenotrophomonas* sp. Exhibited strong uranium tolerance and excellent adsorption performance of uranium, which makes it practical for the treatment of uranium contamination in water.

## Credit author statement

**Zhongqiang Hu:** Conceptualization; Methodology; Formal analysis; Data curation; Experimentation; Writing – original draft: **Zhongkui Zhou:** Formal analysis; Conceptualization; Methodology; Supervision; Writing – review & editing; Funding acquisition: **Yaoyu Zhou:** Formal analysis; Conceptualization; Supervision; Writing – review & editing: **Lili Zheng:** Conceptualization; Methodology; Formal analysis; Data curation; Visualization: **Jianping Guo:** Experimentation: **Yong Liu:** Experimentation: **Zhanxue Sun:** Writing – review & editing: **Zhihui Yang:** Writing – review & editing: **Xiaoxia Yu:** Writing – review & editing.

## Declaration of competing interest

The authors declare that they have no known competing financial interests or personal relationships that could have appeared to influence the work reported in this paper.

## Data availability

Data will be made available on request.

## Acknowledgments

This study was financially supported by the National Natural Science Foundation of China (Grant No. 41662024 and 51709103), Key project of Jiangxi Provincial Key Research and Development Program (Grant Nos. 20212BBG71011), Natural Science Foundation of Hunan Province, China (Grant Nos. 2018JJ3242 and 2021JJ30362), Science and Technology Innovation Leading Plan of High Tech Industry in Hunan Province (Grant No. 2021GK4055).

## Appendix A. Supplementary data

Supplementary data to this article can be found online at https://doi.org/10.1016/j.envres.2022.115093.

## References

Achbergerová, L., Nahálka, J., 2011. 'Polyphosphate - an ancient energy source and active metabolic regulator. Microb. Cell Factories 10, 63-63.
Ahmed, W., Nunez-Delgado, A., Mehmood, S., Ali, S., Qaswar, M., Shakoor, A., Chen, D. Y., 2021. 'Highly efficient uranium (VI) capture from aqueous solution by means of a hydroxyapatite-biochar nanocomposite: adsorption behavior and mechanism. Environ. Res. 201, 111518.
Ashrap, P., Watkins, D.J., Mukherjee, B., Boss, J., Richards, M.J., Rosario, Z., Velez-Vega, C.M., Alshawabkeh, A., Cordero, J.F., Meeker, J.D., 2020. 'Predictors of urinary and blood Metal(loid) concentrations among pregnant women in Northern Puerto Rico. Environ. Res. 183, 109178.
Banala, Uday Kumar, Nilamadhab Prasad Indradyumna Das, and Subba Rao Toleti, 2021. Microbial Interactions with Uranium: towards an Effective Bioremediation Approach. Environmental Technology & Innovation, p. 21.
Bjorklund, G., Christophersen, O.A., Chirumbolo, S., Selinus, O., Aaseth, J., 2017. 'Recent aspects of uranium toxicology in medical geology. Environ. Res. 156, 526–533.
Bondici, V.F., Khan, N.H., Swerhone, Gdw, Dynes, J.J., Lawrence, J.R., Yergeau, E., Wolfaardt, G.M., Warner, J., Korber, D.R., 2015. 'Biogeochemical activity of microbial biofilms in the water column overlying uranium mine tailings. J. Appl. Microbiol. 117, 1079–1094.
Cheng, Y., Li, F., Liu, N., Lan, T., Yang, Y., Zhang, T., Liao, J., Qing, R., 2021. 'A novel freeze-dried natural microalga powder for highly efficient removal of uranium from wastewater. Chemosphere 282, 131084.
Choudhary, Sangeeta, Sar, Pinaki, 2011. 'Uranium biomineralization by a metal resistant Pseudomonas aeruginosa strain isolated from contaminated mine waste. J. Hazard Mater. 186, 336–343.
Coelho, E., Reis, T.A., Cotrim, M., Rizzutto, M., Correa, B., 2020. 'Bioremediation of water contaminated with uranium using Penicillium piscarium. Biotechnol. Prog. 36, e30322.
Deng, S., Ting, Y.P., 2005. 'Characterization of PEI-modified biomass and biosorption of Cu(II), Pb(II) and Ni(II). Water Res. 39, 2167–2177.
Desai, C., Jain, K., Madamwar, D., 2008. 'Evaluation of in vitro Cr(VI) reduction potential in cytosolic extracts of three indigenous Bacillus sp. isolated from Cr(VI) polluted industrial landfill. Bioresour. Technol. 99, 6059–6069.
Ge, S., Ge, S., Zhou, M., Dong, X., 2015. Bioremediation of hexavalent chromate using permeabilized Brevibacterium sp. and Stenotrophomonas sp. cells. J. Environ. Manag. 157, 54–59.
Gerber, U., Hubner, R., Rossberg, A., Krawczyk-Barsch, E., Merroun, M.L., 2018. 'Metabolism-dependent bioaccumulation of uranium by Rhodosporidium toruloides isolated from the flooding water of a former uranium mine. PLoS One 13, e0201903.
Han, Xu, Wong, Yuk Shan, Wong, Ming Hung, Nora Fung Yee Tam, 2007. 'Biosorption and bioreduction of Cr(VI) by a microalgal isolate, Chlorella miniata. J. Hazard Mater. 146, 65–72.
Hao, X., Wang, Q., Zhang, X., Cao, Y., van Mark Loosdrecht, C.M., 2009. Experimental evaluation of decrease in bacterial activity due to cell death and activity decay in activated sludge. Water Res. 43, 3604–3612.
Huang-Lee Llh, D. T. Cheung, Nimni, M.E., 2010. 'Biochemical changes and cytotoxicity associated with the degradation of polymeric glutaraldehyde derived crosslinks. J. Biomed. Mater. Res. 24.
Huang, Feng-Yu, Zhang, Hai-Ling, Wang, Yong-Peng, Yi, Fa-Cheng, Su, Feng, Huang, He-Xiang, Cheng, Meng-Xi, Cheng, Juan, , Wen-Juan Yuan, Zhang, Jie, 2020. 'Uranium speciation and distribution in Shewanella putrefaciens and anaerobic granular sludge in the uranium immobilization process. J. Radioanal. Nucl. Chem. 326, 393–405.
Ishag, A., Li, Y., Zhang, N., Wang, H., Guo, H., Mei, P., Sun, Y., 2020. 'Environmental application of emerging zero-valent iron-based materials on removal of radionuclides from the wastewater: a review. Environ. Res. 188, 109855.
Jain, Monika, Garg, V.K., Kadirvelu, K., 2009. 'Chromium(VI) removal from aqueous system using Helianthus annuus (sunflower) stem waste. J. Hazard Mater. 162, 365–372.
Jing, Y., Du, J., Xie, S., Du, K., Song, J., Lv, Z., 2011. 'Study on Biosorption of Heavy Metal Ion-Uranium by Citrobacter freudii.
Kamunda, C., Mathuthu, M., Madhuku, M., 2016. 'An assessment of radiological hazards from gold mine tailings in the Province of gauteng in South Africa. Int. J. Environ. Res. Publ. Health 13.
Lee, Ji-Hoon, Hur, Hor-Gil, 2014. 'Intracellular uranium accumulation by Shewanella sp. HN-41 under the thiosulfate-reducing condition. Journal of the Korean Society for Applied Biological Chemistry 57, 117–121.
Li, J., Zhang, Y., 2012. 'Remediation technology for the uranium contaminated environment: a review. Procedia Environmental Sciences 13, 1609–1615.
Li, X., Ding, C., Liao, J., Du, L., Sun, Q., Yang, J., Yang, Y., Zhang, D., Tang, J., Liu, N., 2016. Bioaccumulation characterization of uranium by a novel Streptomyces sporoverrucosus dwc-3. J. Environ. Sci. (China) 41, 162–171.
Liu, L., Chen, J., Liu, F., Song, W., Sun, Y., 2021. 'Bioaccumulation of uranium by Candida utilis: investigated by water chemistry and biological effects. Environ. Res. 194, 110691.
Lutke, L., Moll, H., Bernhard, G., 2012. 'Insights into the uranium(VI) speciation with Pseudomonas fluorescens on a molecular level. Dalton Trans. 41, 13370–13378.
Manobala, T., Sudhir, K., Shukla, T., Subba, Rao, Dharmendira Kumar, M., 2019. 'Uranium Sequestration by Biofilm-Forming Bacteria Isolated from Marine Sediment Collected from Southern Coastal Region of India, vol. 145. International Biodeterioration & Biodegradation.
Marqués, A.M., Roca, X., Simon-Pujol, M.D., Fuste, M.C., Congregado, F., 1991. 'Uranium accumulation by Pseudomonas sp. EPS-5028. Appl. Microbiol. Biotechnol. 35, 406–410.
Milacic, S., Petrovic, D., Jovicic, D., Kovacevic, R., Simic, J., 2004. 'Examination of the health status of populations from depleted-uranium-contaminated regions. Environ. Res. 95, 2–10.
Mohamed, Zakaria A., 2001. 'Removal of cadmium and manganese by a non-toxic strain of the freshwater cyanobacterium Gloeothece magna. Water Res. 35, 4405–4409.
Morel, M.A., Ubalde, M.C., Olivera III ravo, Silvia, allejas, C.C., Gill, P.R., Castrolog owinski, Susana, 2009. Cellular and biochemical response to Cr(VI) in Stenotrophomonas sp. FEMS (Fed. Eur. Microbiol. Soc.) Microbiol. Lett. 291.
Nair, R.N., Sunny, F., Manikandan, S.T., 2010. 'Modelling of decay chain transport in groundwater from uranium tailings ponds. Appl. Math. Model. 34, 2300–2311.
Pan, X., Chen, Z., Chen, F., Cheng, Y., Lin, Z., Guan, X., 2015. 'The mechanism of uranium transformation from U(VI) into nano-uramphite by two indigenous Bacillus thuringiensis strains. J. Hazard Mater. 297, 313–319.
Pibil, Stanislav, Marvan, Petr, 1975. 'Accumulation of uranium by the chlorococcal alga. Algological Studies/Archiv für Hydrobiologie 15, 214–225. Supplement Volumes.
Pinel-Cabello, M., Jroundi, F., Lopez-Fernandez, M., Geffers, R., Jarek, M., Jauregui, R., Link, A., Vilchez-Vargas, R., Merroun, M.L., 2021. 'Multisystem combined uranium resistance mechanisms and bioremediation potential of Stenotrophomonas bentonitica BII-R7: transcriptomics and microscopic study. J. Hazard Mater. 403, 123858.
Ramrakhiani, L., Ghosh, S., Majumdar, S., 2016. 'Surface modification of naturally available biomass for enhancement of heavy metal removal efficiency, upscaling prospects, and management aspects of spent biosorbents: a review. Appl. Biochem. Biotechnol. 180, 41–78.
Sanchez-Castro, I., Martinez-Rodriguez, P., Abad, M.M., Descostes, M., Merroun, M.L., 2021. 'Uranium removal from complex mining waters by alginate beads doped with cells of Stenotrophomonas sp. Br8: novel perspectives for metal bioremediation. J. Environ. Manag. 296, 113411.
Sanchez-Castro, I., Martinez-Rodriguez, P., Jroundi, F., Solari, P.L., Descostes, M., Merroun, M.L., 2020. 'High-efficient microbial immobilization of solved U(VI) by the Stenotrophomonas strain Br8. Water Res. 183, 116110.
Sarma, B., Acharya, C., et al., 2014. 'Plant growth promoting and metal bioadsorption activity of metal TolerantPseudomonas aeruginosaIsolate characterized from uranium ore deposit. Proc. Indian Natl. Sci. Acad. Part B Biol. Sci. 84, 157–164.
Saueia, Chr, Mazzilli, B.P., 2006. 'Distribution of natural radionuclides in the production and use of phosphate fertilizers in Brazil. J. Environ. Radioact. 89, 229–239.
Sharma, A., Kaur, J., Lee, S., Park, Y.S., 2016. 'RAPD typing of Lactobacillus brevis isolated from various food products from Korea. Food Sci. Biotechnol. 25, 1651–1655.
Shen, Yanghao, Zheng, Xinyan, Wang, Xiaoyu, Wang, Tieshan, 2018. The biomineralization process of uranium(VI) by Saccharomyces cerevisiae — transformation from amorphous U(VI) to crystalline chernikovite. Appl. Microbiol. Biotechnol.
Sivaperumal, P., Kamala, K., Subramanian, K., Aruni, W., Shanmugam, R., Rajaram, R., 2022. 'Baseline assessment of marine actinobacterial diversity around the nuclear power plant sites, India and its application to uranium remediation. Environ. Res. 212, 113135.
Soni, S.K., Singh, R., Awasthi, A., Singh, M., Kalra, A., 2013. 'In vitro Cr(VI) reduction by cell-free extracts of chromate-reducing bacteria isolated from tannery effluent irrigated soil. Environ. Sci. Pollut. Res. Int. 20, 1661–1674.
Sultan, S., Hasnain, S., 2007. Reduction of toxic hexavalent chromium by Ochrobactrum intermedium strain SDCr-5 stimulated by heavy metals. Bioresour. Technol. 98, 340–344.
Sumit, K., Soni, Rakshapal, , Singh, Ashutosh, Awasthi, Mangal, Singh, Alok, 2013. In Vitro Cr(VI) Reduction by Cell-free Extracts of Chromate-Reducing Bacteria Isolated from Tannery Effluent Irrigated Soil. Environmental Science & Pollution Research.
Suzuki, Yohey, Banfield, Jillian F., 2004. 'Resistance to, and accumulation of, uranium by bacteria from a uranium-contaminated site. Geomicrobiol. J. 21, 113–121.
Tunali, Sibel, Çabuk, Ahmet, Akar, Tamer, 2006. 'Removal of lead and copper ions from aqueous solutions by bacterial strain isolated from soil. Chem. Eng. J. 115, 203–211.
Vieira, L.C., de Araujo, L.G., de Padua Ferreira, R.V., da Silva, E.A., Canevesi, R.L.S., Marumo, J.T., 2019. 'Uranium biosorption by lemna sp. and Pistia stratiotes. J. Environ. Radioact. 203, 179–186.

Wagner, S.E., Burch, J.B., Bottai, M., Pinney, S.M., Puett, R., Porter, D., Vena, J.E., Hebert, J.R., 2010. 'Hypertension and hematologic parameters in a community near a uranium processing facility. Environ. Res. 110, 786–797.
Wang, J., 2002. 'Biosorption of copper(II) by chemically modified biomass of Saccharomyces cerevisiae. Process Biochemistry 37, 847–850.
Wang, Peng, Tan, Kaixuan, Li, Yongmei, Xiao, Wenzhou, Liu, Zhenzhong, Tan, Wanyu, Xu, Yang, 2022. 'The adsorption of U(VI) by albite during acid in-situ leaching mining of uranium. J. Radioanal. Nucl. Chem. 331, 2185–2193.
Wang, T., Zheng, X., Wang, X., Lu, X., Shen, Y., 2017. 'Different biosorption mechanisms of Uranium(VI) by live and heat-killed Saccharomyces cerevisiae under environmentally relevant conditions. J. Environ. Radioact. 167, 92–99.
Yang, J., Volesky, B., 1999. 'Biosorption of uranium on Sargassum biomass. Water Res. 33, 3357–3363.
Ye, Jinshao, Yin, Hua, Xie, Danping, Peng, Hui, Huang, Jie, Liang, Wenyu, 2013. Copper biosorption and ions release by Stenotrophomonas maltophilia in the presence of benzo[a]pyrene. Chem. Eng. J. 219, 1–9.
Yi, Z.J., Yao, J., Zhu, M.J., Chen, H.L., Wang, F., Liu, X., 2017. 'Uranium biosorption from aqueous solution by the submerged aquatic plant Hydrilla verticillata. Water Sci. Technol. 75, 1332–1341.
Yu, Q., Yuan, Y., Feng, L., Sun, W., Lin, K., Zhang, J., Zhang, Y., Wang, H., Wang, N., Peng, Q., 2022. 'Highly efficient immobilization of environmental uranium contamination with Pseudomonas stutzeri by biosorption, biomineralization, and bioreduction. J. Hazard Mater. 424, 127758.
Zhang, Xin, Zhu, Yongguan, Zhang, Yuebin, Liu, Yunxia, Liu, Shaochun, Guo, Jiawen, Li, Rudan, Wu, Songlin, Chen, Baodong, 2014. 'Growth and metal uptake of energy sugarcane (Saccharum spp.) in different metal mine tailings with soil amendments. J. Environ. Sci. 26, 1080–1089.
Zhang, Y., Li, Y., Ning, Y., Liu, D., Tang, P., Yang, Z., Lu, Y., Wang, X., 2018. 'Adsorption and desorption of uranium(VI) onto humic acids derived from uranium-enriched lignites. Water Sci. Technol. 77, 920–930.
Zheng, Xin Yan, Wang, Xiao Yu, Yang Hao, Shen, Lu, Xia, Wang, Tie Shan, 2017. 'Biosorption and biomineralization of uranium(VI) by Saccharomyces cerevisiae —crystal formation of chernikovite. Chemosphere 175, 161–169.
Zou, L., Chen, Z., Zhang, X., Liu, P., Li, X., 2014. 'Phosphate promotes uranium (VI) adsorption in Staphylococcus aureus LZ-01. Lett. Appl. Microbiol. 59, 528–534.